

Optical absorption and its changes due to deformation in molybdenum

M. M. Kirillova, V. Yu. Trubitsyn, A. B. Shaikin, and V. P. Shirokovskii

*Institute of Metal Physics, Ural Scientific Center, Academy of Sciences of the USSR, Sverdlovsk and
Physicotechnical Institute, Ural Scientific Center, Academy of Sciences of the USSR, Sverdlovsk*
(Submitted 17 October 1986)

Zh. Eksp. Teor. Fiz. **93**, 605–612 (August 1987)

The piezoreflection spectra of a molybdenum single crystal were investigated in the photon energy range $\hbar\omega = 0.5\text{--}4.7$ eV and the changes in the optical conductivity as a result of the bulk $\Delta\sigma_1$, tetragonal $\Delta\sigma_3$, and trigonal $\Delta\sigma_5$ elastic deformations were determined. The Green's function method was used in the nonrelativistic approximation to calculate the frequency dependence of the optical conductivity $\sigma(\omega)$ and its change $\Delta\sigma_1(\omega)$ as a result of bulk deformation of a crystal amounting to $\Delta a/a = 0.01$. Allowance for the matrix element of the relevant transition improved greatly the agreement between the experimental and theoretical $\sigma(\omega)$ and $\Delta\sigma_1(\omega)$ curves, and made it possible to explain the frequency dependences of these functions found experimentally.

Interpretation of optical properties of *d* transition metals based on calculations of the energy band structures of specific materials has advanced greatly in recent years. The theory of the energy bands of metals makes it possible to calculate several of their physical characteristics, particularly the frequency dependence of the complex permittivity $\varepsilon(\omega)$, where ω is the angular frequency of the optical wave. Calculations of the function $\varepsilon(\omega)$ in the approximation in which the matrix element of a transition is constant have been carried out for almost all the *d* metals with the cubic lattice. A detailed description of the optical properties of a metal allowing for the energy dependence of the matrix element of a transition is a more difficult task. Such calculations of $\varepsilon(\omega)$ have been carried out already for many metals belonging to this group (Fe, Ni, Cr (Refs. 1–3), V (Refs. 3 and 4), Nb and Mo (Ref. 5)]. Calculations of the optical conductivity $\sigma(\omega)$ of all the metals in the 4*d* period were reported in Ref. 6 for the photon energy range $\hbar\omega \leq 50$ eV. Detailed behavior of the low-frequency interband conductivity of V, Nb, Mo, Rh, and Pd in the range $\hbar\omega < 0.7$ eV was described in Ref. 7. In these investigations the experimental and theoretical data on the dispersion of the complex permittivity $\varepsilon(\omega)$ were obtained for the equilibrium crystal lattice parameters.

Investigations of galvanomagnetic and optical properties of a metal under pressure provide quantitative information on changes in the energy band spectrum [including the shape and dimensions of the Fermi surface, and the deformation shift of the dispersion curves $E(\mathbf{k})$] and open up new opportunities for checking and refinement of various theoretical models of the energy bands of crystals. The effects of pressure on optical properties of a metal are being investigated using uniaxial elastic stresses applied to a crystal along selected axes. Uniaxial stresses alter not only the crystal lattice parameters, but the lattice symmetry, so that this method can provide information on the influence of both bulk and shear deformations on the optical and electron spectra.

We shall report the first investigation of the piezoreflection spectra of a molybdenum single crystal and a determination of changes in its optical conductivity due to bulk ($\Delta\sigma_1$), tetragonal ($\Delta\sigma_3$), and trigonal ($\Delta\sigma_5$) deformations in the photon energy range $\hbar\omega = 0.5\text{--}4.7$ eV. The task of the theoretical investigation was to use a single model of the

band spectrum obtained by the Green's function method in explaining the dispersion of the optical interband conductivity $\sigma(\omega)$ of molybdenum and its changes as a result of bulk deformation $\Delta\sigma_1(\omega)$, and also to analyze the role of the matrix element of a transition in the formation of the spectral dependence of these functions. A theoretical calculation of the function $\Delta\sigma_1(\omega)$ of molybdenum was made for the first time.

1. EXPERIMENTAL DATA

The spectra of the piezoreflection $\Delta R/R$ (R is the reflectivity) were investigated in the photon energy range $\hbar\omega = 0.5\text{--}4.7$ eV using oriented Mo single crystals. The spectra were recorded using automated apparatus.⁸ The bending amplitude of the sample was 10^{-4} .

The optical constants (refractive index n and the extinction coefficient k) were determined by the Beattie polarimetric method in the photon energy range $\hbar\omega = 2.48\text{--}4.96$ eV for the (100) crystallographic plane. The results supplemented our earlier values of n and k also found for a single crystal.⁹ The numerical values of the refractive index and the extinction coefficient were used to calculate the optical conductivity $\sigma = nk\omega/2\pi$. The error in the determination of n and k was 2%, whereas that in $\Delta R/R$ was 5%. Samples were cut from the same single crystal with the electrical resistivity ratio $\rho_{295\text{ K}}/\rho_{4.2\text{ K}} = 10^3$. The orientations of the crystallographic planes were checked by x-ray diffraction. A specularly reflecting surface with class 14 finish was obtained by electropolishing.⁹

The spectra of the piezoreflection $\Delta R/R$ of molybdenum determined for stresses along the [100] and [111] crystallographic axes and normal incidence of light on a sample are plotted in Fig. 1. As before,⁸ a positive value of $\Delta R/R$ was taken to correspond to the increase in the reflection as a result of a tensile stress applied along the selected axis.

The values of $\Delta R/R$ and the elastic constants $s_{11} = 0.263 \times 10^{-11}$ m²/N, $s_{12} = -0.068 \times 10^{-11}$ m²/N, and $s_{44} = 0.917 \times 10^{-11}$ m²/N (Ref. 10) were used in determination of three irreducible components of the piezoreflection tensor whose combinations made it possible to determine the relative increase in the reflection coefficient of light

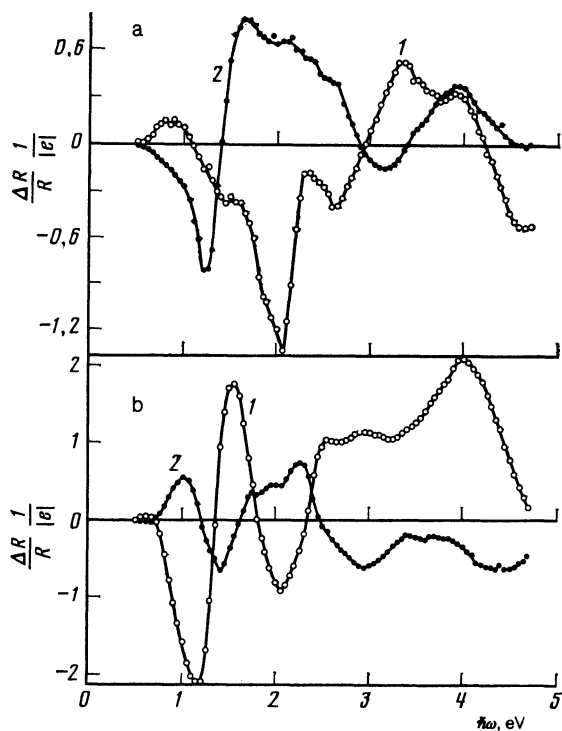


FIG. 1. Piezoreflection spectra of molybdenum reduced to the deformation e for stresses along the [111] (a) and [100] (b) axes: a1) $E \parallel [111]$; a2) $E \perp [111]$; b1) $E \parallel [100]$; b2) $E \perp [100]$ (E is the electric vector of a plane-polarized optical wave).

as a result of bulk (Q_1), tetragonal (Q_3), and trigonal (Q_5) deformations. The dispersion dependences $Q_i(\omega)$ are plotted in Fig. 2. The graphs of $\Delta R/R$ and Q_i (Figs. 1 and 2) demonstrate strong polarizations and orientation effects in the optical properties of molybdenum subjected to uniaxial stresses.

The changes in the optical conductivity as a result of bulk ($\Delta\sigma_1$), tetragonal ($\Delta\sigma_3$), and trigonal ($\Delta\sigma_5$) basal de-

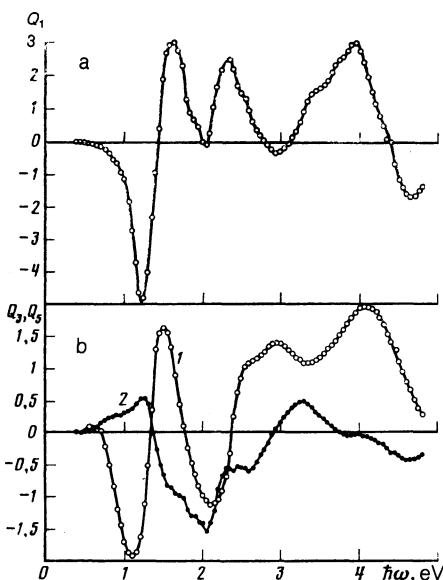


FIG. 2. Frequency dependences of the components of the piezoreflection tensor of molybdenum: a) Q_1 ; b) Q_3 (1) and Q_5 (2).

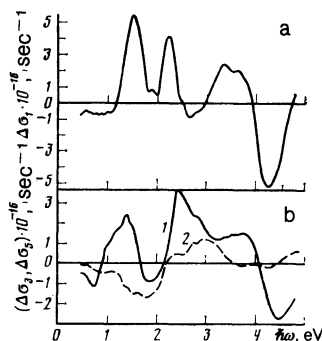


FIG. 3. Changes in the optical conductivity of molybdenum as a result of bulk and shear deformations: a) $\Delta\sigma_1$; b) $\Delta\sigma_3$ (1) and $\Delta\sigma_5$ (2).

formations of a crystal were determined from the values of Q_i and from the optical constants by the Kramers-Kronig transformations. The components $\Delta\sigma_i(\omega)$ are plotted in Fig. 3. The curve $\Delta\sigma_1$ has clear positive structures at energies 1.55 and 2.25 eV, a wide band in the spectral range 3.0–3.4 eV, and a negative structure with a maximum at 4.25 eV. The spectral dependence of the function $\Delta\sigma_3$ is similar to the $\Delta\sigma_1$ curve because of the presence of two strong positive bands at 1.4 and 2.4 eV, a wide "plateau" in the region 3.2–4.0 eV, and a negative structure at $\hbar\omega = 4.5$ eV (Fig. 3b). The $\Delta\sigma_5$ curve differs greatly from $\Delta\sigma_1$ and $\Delta\sigma_3$ primarily because of the smallness of the effect and its almost complete absence in the spectral intervals 0.5–1.2 and 3.5–4.7 eV.

The structures in the $\Delta\sigma_i(\omega)$ curve form as a result of deformation-induced shifts of the energy bands and also because of partial lifting of the degeneracy of the electron states (in the case of shear deformations). We need to carry out theoretical calculations of the functions $\Delta\sigma_i(\omega)$ for given types of deformation in order to interpret the experimental data. We shall calculate the optical conductivity σ of molybdenum for the normal crystal lattice parameter (bcc structure) and the change in the conductivity $\Delta\sigma_1$ due to bulk deformation. We shall then discuss the results obtained for σ and $\Delta\sigma_1$.

2. DISCUSSION OF RESULTS

1. Electron spectrum and its change as a result of deformation

A calculation of the electron spectrum of molybdenum was made by the Green's function method in the nonrelativistic approximation with an l -dependent model potential. This potential¹¹ has one fitting parameter d_l , representing the screening radius of electrons of a given type, for each value of l . In our calculations we selected the following values of d_l : $d_0 = 0.750$; $d_1 = 0.760$; $d_2 = 0.755$; $d_3 = 0.760$. The values of some of the energy terms obtained in this way are listed in Table I together with the data of Ref. 12.

The change in the electron spectrum of molybdenum as a result of deformation was calculated in accordance with Ref. 13. In this approach the theory has an l -dependent parameter η_l representing the change in the screening radii as a result of deformation. In fact, $\eta_l = 0$ corresponds to the case when d_l follows the changes in the lattice parameter a in such a way that the ratio d_l/a remains constant; if $\eta_l = 1$, the screening radius is constant. Table I gives the energy derivatives $a \partial E / \partial a$ calculated for $\eta_0 = \eta_1 = \eta_3 = 0$ and

TABLE I. Energy values (Ry) at high-symmetry points of Brillouin zone of molybdenum and their derivatives with respect to bulk deformation.

term	E (k)	E (k) [11]	$\alpha \partial E (k) / \partial \alpha$	term	E (k)	E (k) [12]	$\alpha \partial E (k) / \partial \alpha$
Γ_1	0.314	0.318	-2.573	N_1	0.429	0.434	-1.499
$\Gamma_{25'}$	0.724	0.726	-2.445	N_2	0.574	0.578	-1.742
Γ_{12}	0.914	0.914	-3.303	N_1'	0.906	0.923	-4.105
H_{12}	0.339	0.403	-1.005	N_1	0.929	0.929	-3.485
$H_{25'}$	1.091	1.091	-4.299	N_4	0.965	0.967	-3.640
P_4	0.617	0.627	-2.417	N_3	1.142	1.143	-4.597
P_3	0.973	0.975	-3.692				

$\eta_2 = 0.3$. Selection of a nonzero parameter η_2 is explained by the stronger localization of the *d*-type states within a muffin-tin sphere. Test calculations showed also that the change in η_3 corresponding to *f* electrons has practically no effect on the derivatives $\alpha \partial E / \partial \alpha$.

2. Optical conductivity

We calculated the frequency dependence of the optical conductivity $\sigma(\omega)$ by the method of tetrahedra. The optical conductivity of molybdenum found in the approximation of a constant matrix element of a transition for the equilibrium value of the lattice parameter is plotted in Fig. 4a; this figure includes also the experimental data obtained in Ref. 9 and those obtained by us in the present study. A comparison of the graphs of σ shows that there are several differences between the experimental and theoretical results. For example, the experimental $\sigma(\omega)$ curve has two clear maxima, *B* and *C*, in the energy range $\hbar\omega > 1.0$ eV, located at 2.5 and 4.0 eV; the second of these is stronger than the first (we shall ignore the range of energies below 1.0 eV because relativistic effects are important at these energies). In the theoretical curve the maxima *B* and *C* are practically the same and, moreover, there is an additional structure at energies $E > 4.3$

eV with the last maximum at 5.3 eV. It should be noted that a similar structure was also obtained in the calculations reported in Ref. 14.

An analysis of the partial contributions $\sigma_{ij}(\omega)$ of separate pairs of energy bands to the total optical conductivity shows that the main contribution to the structure at 1.9–2.5 eV (peak *B*) comes from electron transitions from the third to the fourth band (3→4). A small peak at 2.7 eV is associated with the 3→6 transitions. The second main maximum of $\sigma(\omega)$ at 4.0 eV (peak *C*) is due to superposition of the contributions from a whole series of band pairs: 3→5, 2→4, 3→6, 3→4. The structure in the range $E > 4.3$ eV is due to the 1→4 and 2→4 transitions. These absorption peaks are not observed in the experimental results. On the whole, a comparison of the experimental and theoretical graphs $\sigma(\omega)$ demonstrates that the frequency dependence of the optical conductivity cannot be described satisfactorily in the constant-matrix-element approximation.

We therefore calculated matrix elements of optical transitions in the dipole approximation. The matrix elements were calculated in accordance with Ref. 15; the technical details of the calculations and an analysis of its precision can be found in Ref. 16. The frequency dependence $\sigma(\omega)$ calculated allowing for the matrix element is plotted in Fig. 4b. We can see that inclusion of the matrix elements has a considerable influence on the structure of the optical conductivity curve. Thus, in full agreement with the experimental results, the main maximum is now at 4.0 eV. The peak at 2.7 eV has disappeared and the amplitudes of the peaks in the range $E > 4.3$ eV have decreased greatly relative to the main maximum, altering radically the structure of the $\sigma(\omega)$ curve in this range.

These changes are due to the following factors. Firstly, inclusion of the matrix elements enhances greatly the contribution of the 3→5 electron transitions compared with the 3→4 transitions. However, the ratio of the contributions made by the 1→4 and 2→4 transitions to the contribution made by the 3→4 transitions remains the same as before. All these changes cause a strong enhancement of the main maximum at 4.0 eV. Secondly, when the matrix elements are included there is a considerable change in the energy dependences of the individual partial contributions $\sigma_{ij}(\omega)$ to the optical conductivity. For example, there is a significant change in the structure of the $\sigma_{ij}(\omega)$ curves in the case of the 1→4, 3→5, 3→6, and 4→5 transitions. In particular, the disappearance of the $\sigma(\omega)$ peak at 2.7 eV is due to the smallness of the matrix element for the 3→6 transitions in this range of energies, although for $E > 3.3$ eV the structure of the partial contribution of these transitions is still retained.

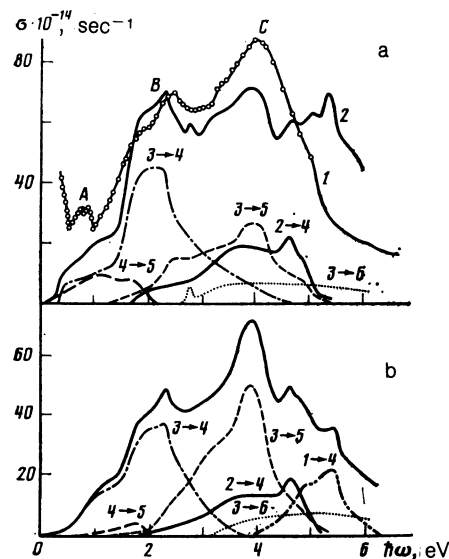


FIG. 4. Optical conductivity σ of molybdenum: a1) experimental results from Ref. 9 and those obtained in the present study; a2) theoretical curve of σ obtained in the approximation of a constant element of transition; b) theoretical curve of σ obtained allowing for the energy dependence of the matrix element. The numbers identify the partial contributions made to the conductivity by pairs of energy bands.

A comparison of our calculated data with the results of calculations of the interband conductivity of Mo made by the LMTO method using a self-consistent crystal potential⁶ shows a close agreement with the $\sigma(\omega)$ theoretical curves. The difference lies in the stronger structure of the peak in the region of 5 eV in the $\sigma(\omega)$ graph obtained in Ref. 6. This peak is strongly flattened in the experimental optical conductivity curve (Fig. 4a).

3. Change in the optical conductivity due to bulk deformation

A calculation of the change in the optical conductivity $a\partial\sigma/\partial a$ as a result of bulk deformation was carried out in accordance with Ref. 8 by computing directly the values of σ for the normal and modified ($\Delta a/a = 0.01$) lattice constants, and then applying numerical differentiation. Figure 5a shows the results of a calculation of $a\partial\sigma/\partial a$ in the constant-matrix-element approximation (this figure includes also the experimental curve), whereas Fig. 5b shows the results obtained allowing for the probabilities of optical transitions in the dipole approximation; in the latter case no allowance is made for a possible change in the matrix element as a result of deformation. As before, only the energy range $E > 1.0$ eV is analyzed.

We shall consider the first variant of the calculation. The agreement between the theoretical and experimental results in the range from 1.2 to 2.4 eV can be regarded as good, because not only the structure but also the positions of its main components are the same (to within 0.05 eV); these components comprise two maxima and minima. We can also regard as satisfactory the agreement of the theory with the experimental results in the range from 3.0 to 4.0 eV. It is meaningless to consider the theoretical results for $E > 4.0$ eV in this approximation because allowance for the energy dependences of the matrix elements becomes important in this part of the spectrum. The greatest discrepancy between the theory and experiment is found in the energy interval 2.5–3.0 eV, where the sign of the experimental curve $\Delta\sigma_1$ is reversed and there is a minimum, whereas the theoretical curve shows two sharp maxima and no reversal of the sign. An analysis of the partial contributions $a\partial\sigma_{ij}/\partial a$ to the frequency dependence

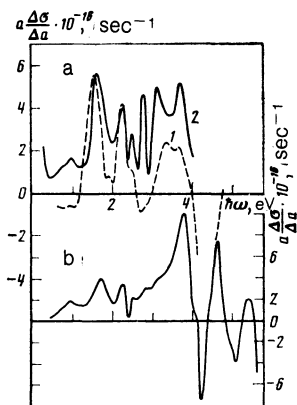


FIG. 5. Changes in the optical interband conductivity of Mo as a result of bulk deformation ($\Delta a/a = 0.01$): a1) experimental results; a2) theoretical $\Delta\sigma_1$ curve obtained in the approximation of a constant matrix element of a transition; b) theoretical $\Delta\sigma_1$ curve obtained allowing for the energy dependence of the matrix element. The numbers identify the partial contributions made to $\Delta\sigma_1$ by pairs of energy bands.

dence of the change in the optical conductivity as a result of bulk deformation (Fig. 5a) shows that the first of these is due to the 3 → 5 transitions and the second due to 3 → 6. Since it is in the case of these electron transitions that the structure of the $\sigma_{ij}(\omega)$ curve in the investigated energy interval changes considerably when an allowance is made for the matrix element, inclusion of the probabilities of optical transitions should suppress these peaks.

In fact, a calculation carried out allowing for the matrix element of a transition alters considerably the whole energy dependence of the function $a\partial\sigma/\partial a$ in the range $\hbar\omega > 2.4$ eV (Fig. 5b). As expected, two false peaks at 2.5 and 2.7 eV have disappeared, but this has not reversed the sign of the function. Moreover, instead of a two-hump structure in the interval 3.0–4.0 eV there is now a giant maximum at 3.8 eV. We can see from Fig. 5b that the reason for the discrepancy between the theoretical and experimental data is most probably an overestimate of the contribution of the 3 → 5 transitions in this range of energies. This may be because of a change in the matrix elements themselves as a result of deformation, but we cannot exclude the possibility that it could simply be due to the relativistic effects. Further refinements of the theory are needed in this range. Inclusion of the matrix elements in the range $E > 4$ eV provides a correct description of the frequency dependence of the function $\Delta\sigma_1(\omega)$: the points of reversal of the sign and the total width of the negative region agree with the experimental data to within 0.1 eV. The "sawtooth" shape of the theoretical curve is associated with the presence of a structure in the calculated optical conductivity $\sigma(\omega)$ (Fig. 4b), which is not manifested in the experimental curve. This has been discussed by us earlier.⁸

CONCLUSIONS

Our calculations of the frequency dependence of the optical conductivity $\sigma(\omega)$ have identified the mechanism responsible for the main absorption band of molybdenum located in the spectral range 0.5–6 eV. The results indicate that the partial contributions to $\sigma(\omega)$ made by the electron 3 → 4 and 3 → 5 transitions between the bands characterized by a mixed ($d-p$) symmetry are the largest. The energy shifts of the same pairs of energy bands under the action of bulk deformation gives rise to the main structures in the $\Delta\sigma_1(\omega)$ curve in the spectral intervals 0.5–2.0 eV (3 → 4) and 3.0–3.5 eV (3 → 5), manifested clearly by the experimental results.

Allowance for the energy dependence of the matrix element of the relevant transition affects the magnitude and spectral dependences of the partial contributions made to the functions $\sigma(\omega)$ and $\Delta\sigma_1(\omega)$ and it improves greatly the agreement between the theoretical and experimental curves. Description of the experimental data on the optical conductivity σ is still unsatisfactory at low frequencies (peak A at 0.9 eV); this is true also of $\Delta\sigma_1$ in the interval 2.5–3.0 eV. We can expect a better agreement between the theory and experiment in these parts of the spectrum if calculations are made of the electron structure of Mo allowing for the relativistic effects, particularly for the spin-orbit interaction.

It should also be pointed out that, according to our data, expansion of the bcc lattice of Mo shifts the energy band $E_i(\mathbf{k})$ downward on the energy scale. The total width of the 4d band, corresponding to the energy gap $H_{25'}-H_{12}$, decreases by 0.45 eV when the lattice deformation is $\Delta a/a$

$a = 0.01$. Interpretation of the frequency dependences of the functions $\Delta\sigma_3(\omega)$ and $\Delta\sigma_5(\omega)$ requires carrying out of similar calculations for the shear deformations.

¹C. S. Wang and J. Callaway, Phys. Rev. B **9**, 4897 (1974).

²D. G. Laurent, J. Callaway, and C. S. Wang, Phys. Rev. B **20**, 1134 (1979).

³Y. Kubo and S. Wakoh, J. Phys. Soc. Jpn. **50**, 835 (1981).

⁴D. G. Laurent, C. S. Wang, and J. Callaway, Phys. Rev. B **17**, 455 (1978).

⁵J. Yamashita, Y. Kubo, and S. Wakoh, J. Phys. Soc. Jpn. **42**, 1906 (1977).

⁶I. I. Mazin, E. G. Maksimov, S. N. Rashkeev, and Yu. A. Uspenskiĭ, Zh. Eksp. Teor. Fiz. **90**, 1092 (1986) [Sov. Phys. JETP **63**, 637 (1986)].

⁷S. N. Rashkeev, Yu. A. Uspenskiĭ, and I. I. Mazin, Zh. Eksp. Teor. Fiz. **88**, 1687 (1985) [Sov. Phys. JETP **61**, 1004 (1985)].

⁸M. M. Kirillova, V. Yu. Trubitsyn, A. V. Shaĭkin, and V. P. Shirokovskiĭ, Fiz. Met. Metalloved. **61**, 876 (1986).

⁹M. M. Kirillova, L. V. Nomerovannaya, and M. M. Noskov, Zh. Eksp. Teor. Fiz. **60**, 2252 (1971) [Sov. Phys. JETP **33**, 1210 (1971)].

¹⁰G. Leibfried and N. Breuer, *Point Defects in Metals. I. Introduction to the Theory*, Springer Verlag, Berlin (1978).

¹¹R. F. Egorov and V. P. Shirokovskiĭ, Fiz. Met. Metalloved. **42**, 217 (1976).

¹²I. Petroff and C. R. Viswanathan, Phys. Rev. B **4**, 799 (1971).

¹³V. P. Shirokovskiĭ, N. A. Shilkova, and V. Yu. Trubitsyn, Fiz. Met. Metalloved. **58**, 42 (1984).

¹⁴W. E. Pickett and P. B. Allen, Phys. Rev. B **11**, 3599 (1975).

¹⁵A. B. Chen, Phys. Rev. B **14**, 2384 (1976).

¹⁶N. A. Shilkova and V. P. Shirokovskiĭ, Deposited Paper No. 2502-V86 [in Russian], VINITI, Moscow (1986).

Translated by A. Tybulewicz